

An Adaptive Mesh Strategy for Transient Flows and Heat Transfer Simulations

Tales Luiz Popiolek

Department of Mathematics, Federal University Foundation of Rio Grande, Av. Itália km 8, 96201-900 Rio Grande, RS, Brazil
dmttales@furg.br

Armando Miguel Awruch

Graduate Program in Civil Engineering, Federal University of Rio Grande do Sul, Av. Osvaldo Aranha 99, 90035-190 Porto Alegre, RS, Brazil
awruch@adufgrs.ufrgs.br

Abstract: An adaptive mesh strategy for the numerical simulation of incompressible transient flows with heat transfer and mass transport is presented in this work. The Finite Element technique, with unstructured meshes formed by tetrahedral elements, and the two-step Taylor-Galerkin method are used. The velocity field is obtained by an explicit scheme, while pressure field is computed by an implicit scheme using a pre-conditioned conjugate gradient method. Error indicators, an adaptation criterion, a refinement scheme, a smoothing process and an appropriate data structure are used to obtain a suitable mesh in order to get accurate results. To evaluate the adaptive mesh strategy performance, two numerical applications involving transient incompressible viscous fluid flows with heat transfer and mass transport, taking into account relevant error indicator, are presented.

Keywords: adaptive mesh, heat transfer, mass transport, incompressible flows, transient flows.

1. INTRODUCTION

A correct discretization of the computational domain, based in the physical phenomena involved in the problem to be analyzed, is necessary to obtain numerical accuracy in the simulation of transient viscous incompressible flow. Frequently simulations begin using an uniform coarse mesh, but a mesh refinement process is applied along time in some regions in order improve numerical accuracy. This refinement procedure is performed simultaneously and iteratively with the numerical solution employing a mesh adaptation strategy, which include error indicators and an adaptation criterion.

Four techniques may be used to improve the finite element mesh: (a) the “h” method, which is characterized by the mesh refinement and/or de-refinement, used by Bank et al. (1983), Bey (1995), Mavriplis (2000), Biswas and Strawn (1994), Connel and Holmes (1994), Löhner (1987) among other authors; (b) the “r” method, which uses a smoothing process, employed by Mavriplis (1995), Ait-Ali-Yahia et al. (1996), Habashi et al. (2000) and Ivanenko and Azarenok (2002) among other authors; (c) the remeshing method, where the mesh is rebuilt completely, used by Peraire et al. (1987), Löhner (1989) and Dannelongue and Tanguy (1990) and partially used by Probert et al. (1991), among other authors; (d) the “p” method, which is based in the shape function improvement (Demkowicz et al., 1991 and Devloo et al., 1988, among other authors).

The main objective of this work is to present an adaptive mesh strategy to improve the accuracy of incompressible transient flow simulations, integrating to the solver a refinement scheme, an adaptation criterion, a mesh smoothing technique and an appropriate data structure. In this context, it is possible to build fixed and dynamic meshes.

To analyze the automatic adaptive mesh strategy, two examples are presented in section 4. They are solved using a semi-implicit finite element Taylor-Galerkin scheme and the pseudo-compressibility hypotheses.

2. THE ADAPTIVE MESH STRATEGY

An adaptive mesh strategy is characterized by an error indicator, an adaptation criterion, a refinement scheme, a smoothing process and a suitable data structure.

The error indicator is used to identify the characteristics and behaviour of the numerical solutions in order to determine regions of the computational domain where a refined mesh is necessary, looking for an accurate solution. Taken in to account the specific applications of this work, an error indicator considering the temperature or the substance concentration gradients is adopted. Additional informations may be found in Argyris et al. (1990) and Popiolek and Awruch (2006).

The adaptation criterion is a consequence of the error indicator analysis. Elements to be refined are identify by the following expression:

$$q_i > (\bar{q} + \alpha q_{sd}) \quad i=1,2,\dots,nel \quad (1)$$

where, i is the element number, nel is the total number of elements, \mathbf{a} is an arbitrary parameter to control qualitatively and quantitatively the refinement scheme, \mathbf{q}_i is the error indicator for i , and \mathbf{q}_{sd} is given by:

$$\mathbf{q}_{sd} = \sqrt{\frac{\sum_{i=1}^{nel} (\mathbf{q}_i - \bar{\mathbf{q}})^2}{nel}} \quad (2)$$

with $\bar{\mathbf{q}}$ being the mean value.

Elements identified to be refined are divided in eight new elements; this type of refinement is defined as a *regular* refinement, and it is represented by 1:8. To close the refinement scheme and to avoid hanging nodes, it is necessary to perform *irregular* refinements in neighbour elements, represented by 1:2, 1:3 or 1:4. Elements having less than four edges divided by new nodes, created as a consequence of the adaptation scheme applied to their neighbour elements, are submitted to *irregular* refinements. However, if an element has four or more edges divided by new nodes, it is submitted to a *regular* refinement. More details may be found in Biswas and Strawn (1994) and Popiolek and Awruch (2006).

In order to avoid distortion of elements (mainly when refinements of the type 1:2, 1:3 or 1:4 are applied), and to obtain a mesh with high quality with respect to the elements geometry, it is necessary to implement a smoothing process, which include node re-allocation. Usually a smart Laplacian smoothing or constrained Laplacian smoothing is employed (see Freitag and Ollivier-Gooch, 1996 and Zhou and Shimada, 2000).

Efficiency of a mesh adaptation strategy is very linked to the data structure, which allows to define and manage the connectivity among the different entities of a mesh (cells, faces, edges and nodes). Data structures were presented by Kollinderis and Vijayan (1993), Biswas and Strawn (1994), Connel and Holmes (1994), Bey (1995), Speares and Berzins (1997) and Grosso et al. (1997) among others. Here the data structure presented by Popiolek and Awruch (2006) was used.

3. THE GOVERNING EQUATIONS

Slightly compressible flows and mass or heat transport are governed by the following system of differential equations:

$$\frac{1}{c^2} \frac{\partial p}{\partial t} + \mathbf{r} \frac{\partial u_i}{\partial x_i} = 0 \quad \text{in } \mathbf{W} \quad (3)$$

$$\frac{\partial}{\partial t} (\mathbf{r} u_i) + \frac{\partial}{\partial x_j} (\mathbf{r} u_i u_j) + \frac{\partial p}{\partial x_j} \mathbf{d}_{ij} - \frac{\partial}{\partial x_j} \left[\mathbf{m} \left(\frac{\partial u_i}{\partial x_j} + \frac{\partial u_j}{\partial x_i} \right) + \mathbf{I} \frac{\partial u_k}{\partial x_k} \mathbf{d}_{ij} \right] - S_{u_i} = 0 \quad \text{in } \Omega \quad (4)$$

$$\frac{\partial}{\partial t} (\mathbf{r} \mathbf{f}) + \frac{\partial}{\partial x_i} (\mathbf{r} u_i \mathbf{f}) - \frac{\partial}{\partial x_i} \left(D_{ij} \frac{\partial \mathbf{f}}{\partial x_j} \right) - S_{\mathbf{f}} = 0 \quad \text{in } \mathbf{W} \quad (5)$$

with the following boundary conditions:

$$u_i = \hat{u}_i \quad \text{in } \mathbf{G}_u \quad (6.a)$$

$$(-p \mathbf{d}_{ij} + \mathbf{t}_{ij}) n_j = \hat{t}_i \quad \text{in } \mathbf{G}_t \quad (6.b)$$

$$\mathbf{f} = \hat{\mathbf{f}} \quad \text{in } \Gamma_{\mathbf{f}} \quad (7.a)$$

$$\left(D_{ij} \frac{\partial \mathbf{f}}{\partial x_i} \right) n_j = \hat{q}_i \quad \text{in } \mathbf{G}_q. \quad (7.b)$$

Initial conditions for u_i , p and \mathbf{f} , at $t = 0$, must be given. In Eq. (3) to Eq. (7), u_i is the velocity component in the direction of the coordinate x_i , p is the pressure, \mathbf{r} is the specific mass, c is the sound speed, \mathbf{m} and \mathbf{I} are the shear and volumetric viscosities, respectively, \mathbf{f} is a scalar quantity (as the temperature or some pollutant concentration), D_{ij} is a

component of the conductivity or dispersion coefficients tensor, S_{u_i} and S_f are, respectively, source terms in the momentum and heat (or mass) transport equations, d_{ij} is the Kroenecker delta, n_j are the cosine of the angle formed by the outflow normal to the boundary and the coordinate axis x_j , \hat{t}_i and \hat{q}_i are components of the surface traction and flux of the scalar quantity, respectively, t_{ij} is a component of the shear stress tensor and t is the time variable. Ω is the problem domain, G_u and G_t are parts of the boundary surface where velocity components \hat{u}_i or tractions \hat{t}_i are prescribed, respectively, and G_f and G_q are parts of the boundary surface where the quantity \hat{f} and flux components \hat{q}_i across the surface are prescribed, respectively. When f is the temperature, convection and/or radiation boundary conditions could be included.

The numerical algorithm is obtained expanding in Taylor series the governing equation and applying after the space discretization process, using the Finite Element Method (FEM) in the context of the classical Budnov-Galerkin scheme.

The critical time step may be calculated with the following expression (Zienkiewicz and Wu, 1992 and Zienkiewicz et al., 1999):

$$\Delta t_{crit} = \frac{\Delta t_s \Delta t_n}{\Delta t_s + \Delta t_n} = \frac{h_E}{|u_E|} \left(\frac{1}{1/Pe+1} \right) \quad (8)$$

being $\Delta t_s = h_E/|u_E|$ and $\Delta t_n = h_E^2/2k$ the stability limits for one dimensional problems with dominant advective and diffusive terms, respectively. In Eq. (8), h_E is a characteristic dimension of a generic element E , $|u_E|$ is the absolute value of the velocity at the center of this element and $Pe = h_E|u_E|/2k$ is the local Peclet number, where k is the diffusive coefficient. Then, taking in to account Eq. (8), it may be adopted $\mathbf{Dt} = \beta \mathbf{Dt}_{crit}$, where β is a safety factor ($\beta < 1.0$).

4. NUMERICAL APPLICATIONS

4.1. Flow around an heated/cooled cylinder

The flow around a heated/cooled cylinder is analyzed. Based in this problem, many other applications of different engineering fields may be studied.

The computational domain, as well as the boundary conditions are shown in Fig. 1, where u_i are the velocity components, p is the pressure, T is the temperature and d is the diameter of the cylinder (in this work $d = 1.0$ is adopted).

Although a two-dimensional flow was simulated in this example, a three-dimensional solver was used to obtain the numerical solution. For this reason, a layer of tetrahedral elements, which width is equal to $0.1d$, was taken in the perpendicular direction to the plane indicated in Fig. 1. Velocity components normal to this plane were prescribed with values equal to zero.

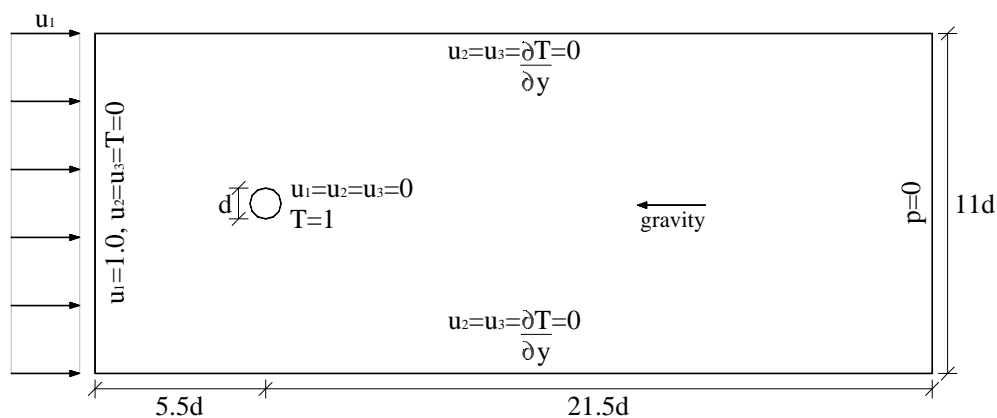


Figure 1. Computational domain and boundary conditions for flow around a heated/cooled cylinder.

For isothermal flows, body force components in the momentum equations, Eq. (4), do not exist. For non isothermal flows, the body (buoyancy) force components are given by:

$$S_{u_i} = \frac{Gr}{Re^2} T^* \mathbf{d}_{i1} = Ri T^* \mathbf{d}_{i1} \quad (9)$$

where Gr and Re are the Grashof number and Reynolds number, respectively, \mathbf{d}_{i1} is the Kroenecker delta and T^* is a dimensionless value, given by:

$$T^* = \frac{T - T_w}{T_w - T_\infty} \quad (10)$$

with T being the local temperature, T_∞ the prescribed temperature of the fluid in the entrance and T_w is the temperature at the wall of the immersed body.

Grashof and Reynolds numbers are given, respectively, by:

$$Gr = \frac{g \mathbf{h} \Delta T d^3}{\mathbf{n}^2} \quad (11)$$

$$Re = \frac{U_\infty d}{\mathbf{n}} \quad (12)$$

where g is the gravity acceleration, \mathbf{h} is the thermal expansion coefficient, $\Delta T = T_w - T_\infty$, d is a characteristic length (in this example, d is the diameter of the cylinder), \mathbf{n} is the kinematics viscosity and U_∞ is the prescribed flow velocity, far from the immersed body.

The Richardson, Prandtl and Peclet numbers are defined, respectively, as follows:

$$Ri = \frac{Gr}{Re^2} \quad (13)$$

$$Pr = \frac{\mathbf{n}}{\mathbf{e}} \quad (14)$$

$$Pe = Pr Re = \frac{U_\infty d}{\mathbf{e}} \quad (15)$$

where $\mathbf{e} = \frac{D}{\mathbf{r} C_p}$ is the thermal diffusivity, D is the thermal conductivity, C_p is the specific heat coefficient at constant pressure and \mathbf{r} is the specific mass.

The initial mesh is shown in Fig. 2 containing 6090 nodes and 17677 tetrahedral elements, with only one layer of elements in the direction of axis z .

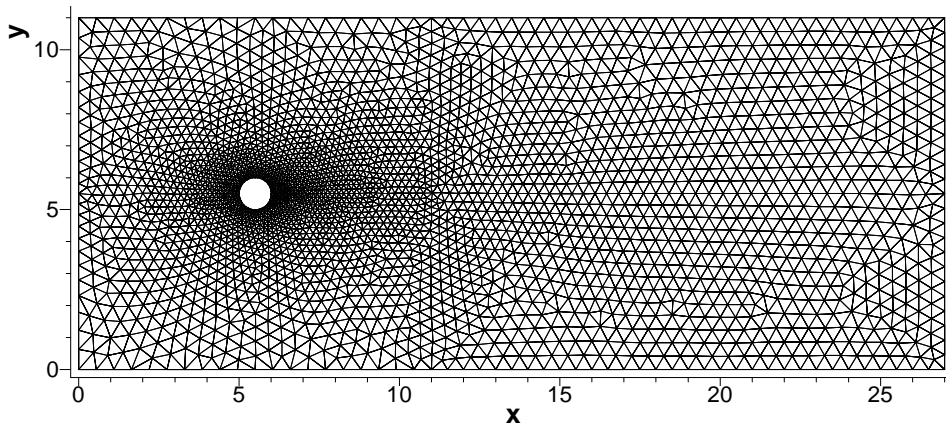


Figure 2. Initial finite element mesh.

To simulate the effects of the heated/cooled cylinder, as in Hatanaka and Kawahara (2000), it was considered Grashof number $Gr = -10000$ and $Gr = 0$, corresponding to values of Richardson number in the interval $Ri = -1.0$ and $Ri = 0.0$. It was adopted $Re = 100$ and $Pr = 0.706$, consequently, $Pe = 70.6$.

The heated cylinder is represented by positive values of Richardson number then the buoyancy force component S_{u_1} and the mainstream have the same direction. The cooled cylinder is represented by negative values of Richardson number then the buoyancy force component S_{u_1} and the mainstream have opposite directions.

Starting from an initial mesh, the transient solution imposes successive mesh updating. Here the mesh was updated each 500 time steps ($\Delta t = 0.0005$ s) using the temperature gradient indicator (see Popiolek and Awruch, 2006) with $\alpha = 0.7$ (see Eq. 1). This criterion presented the best behaviour, identifying correctly regions to be refined.

In Figure 3 and 4 the refined mesh and respective isotherms are presented for $Ri = -1.0$. The sequence for different configurations shown in Fig. 3 and 4, take place with an interval of 2.0 seconds. The error indicator leads to mesh refinements in regions of high temperature gradients located at the whirls and close to the body, which is a very important region with respect to the flow dynamics, where vortex shedding occurs.

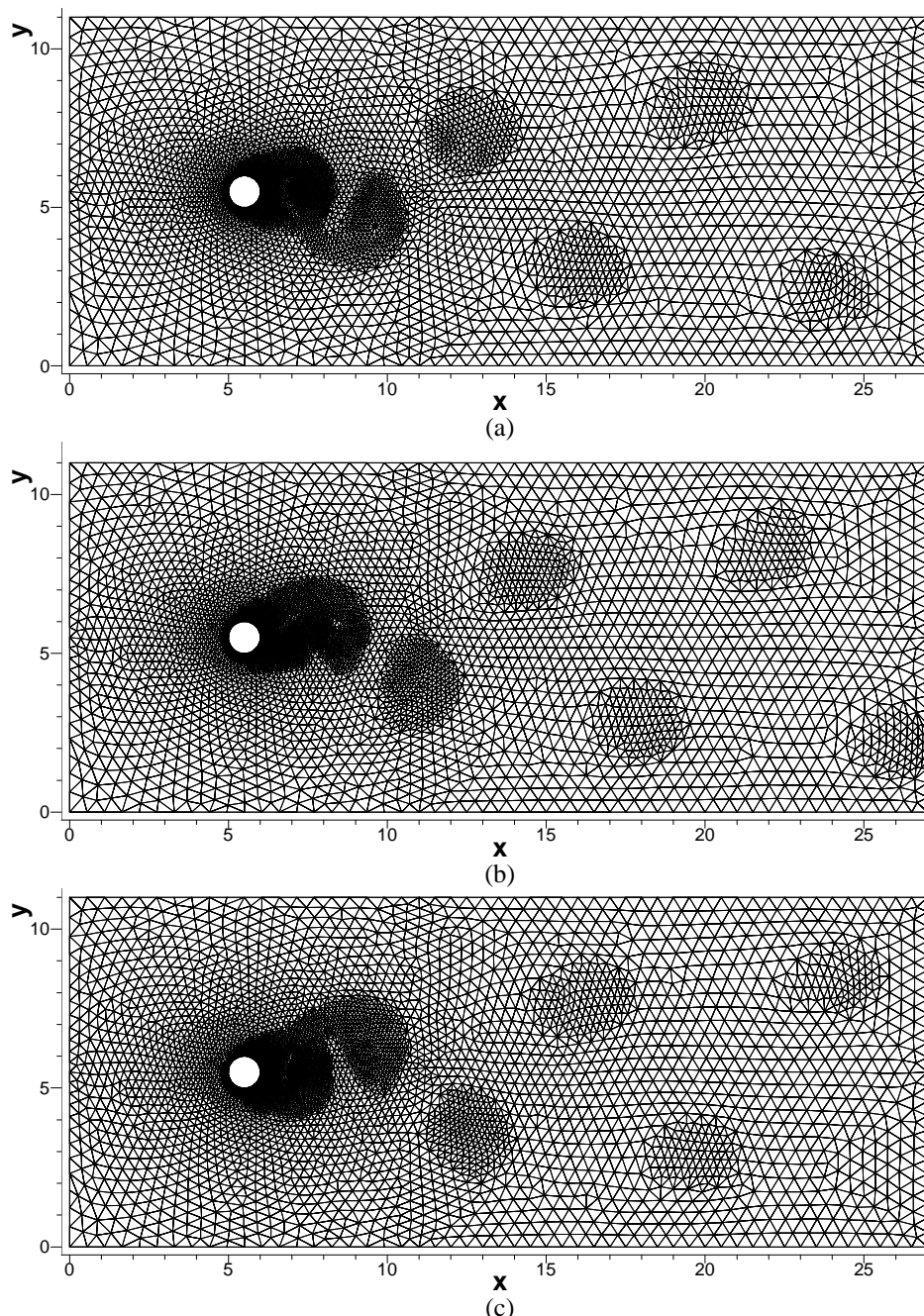


Figure 3. Refined meshes using the error indicator corresponding to the temperature gradient. Sequence (a), (b) and (c) are separated by time intervals equal to 2 seconds.

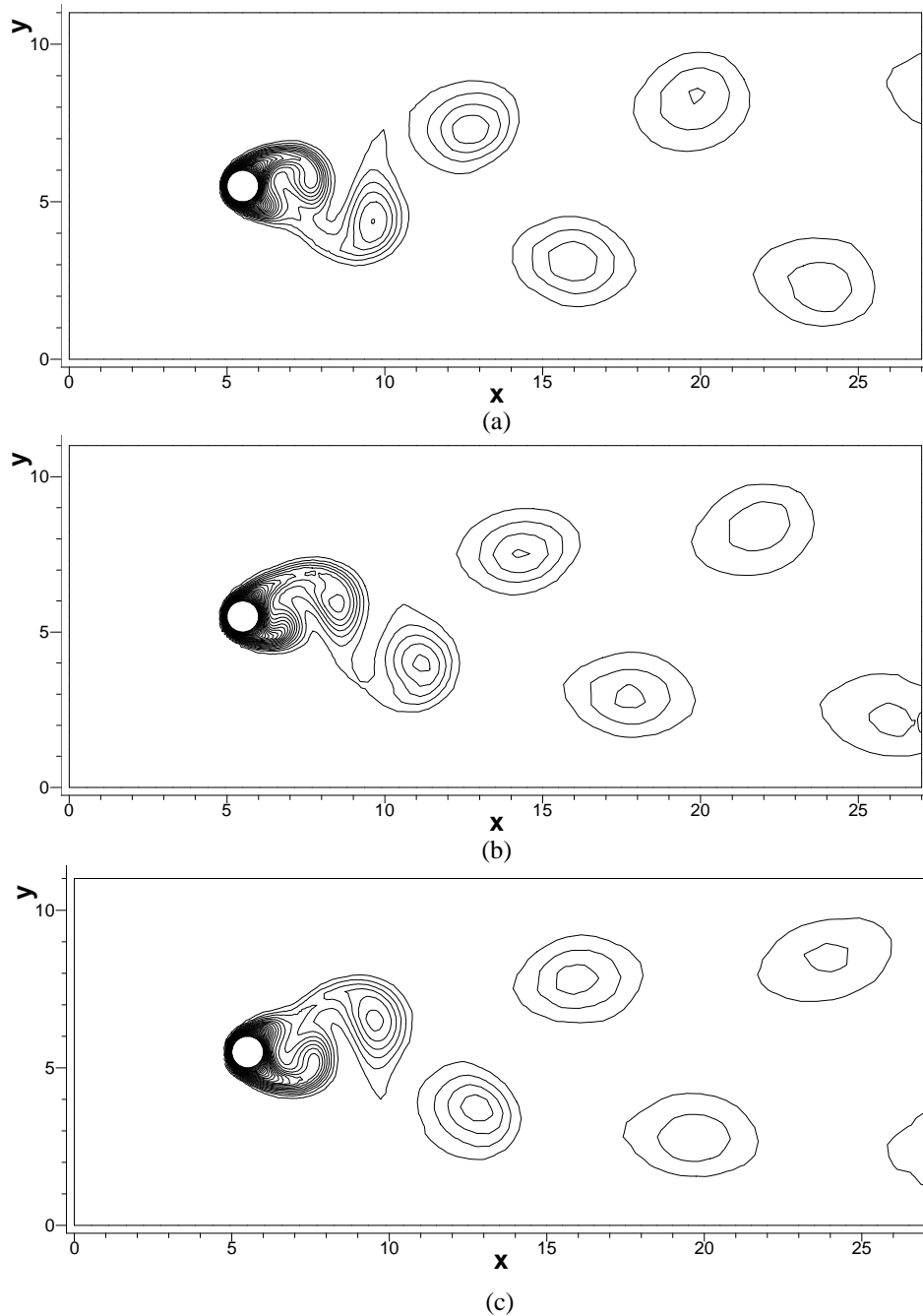


Figure 4. Isotherms calculated with the adaptive mesh strategy given in Fig. 3, for $Ri = -1.0$.

In Figure 5 and 6, streamlines and isotherms corresponding to $Ri = 0.0$ and $Ri = -1.0$ (at the same instant), respectively, are shown.

It can be observed in Fig. 5 that, when $Ri = 0.0$, the von Kármán vortex street is formed, and vortex shedding is periodic. Presence of whirls, with higher temperatures at their centers and moving in the mainstream direction, can be verified in the isotherms. The same phenomenon occurs for other negative values of Ri number.

When Richardson number decreases from 0.0 to -1.0, the von Kármán vortex street is amplified (growing continuously) and whirls displacement with higher temperature at their centers, are more spaced out.

Values of Strouhal numbers (indicating vortex shedding frequencies) equal to 0.129 and 0.178 were obtained for $Ri = -1.0$ and 0.0, respectively. These results are close to those obtained by Hatanaka and Kawahara (1995). As can be observed, vortex shedding intensity increases when Richardson number goes from -1.0 to 0.0.

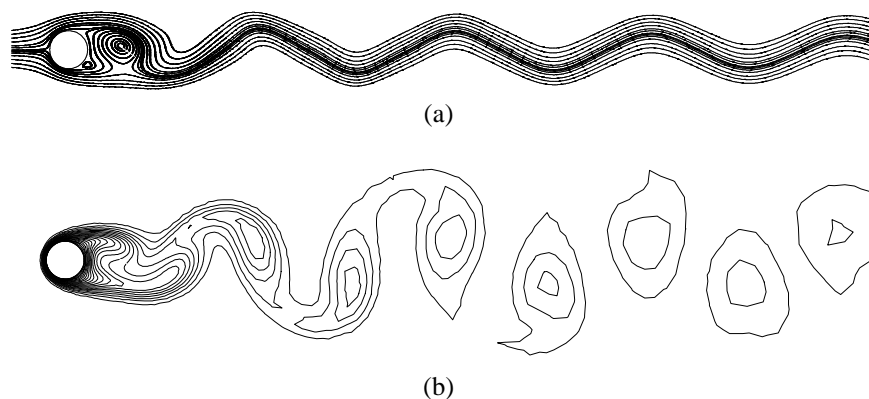


Figure 5. Numerical simulation of the flow around a cylinder for $Ri = 0.0$:
 (a) Streamlines; (b) Isotherms.

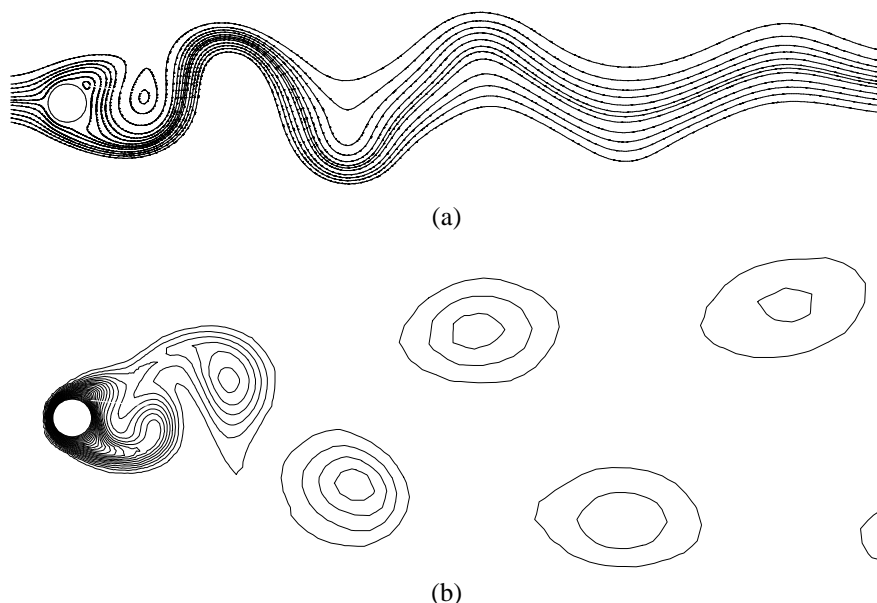


Figure 6. Numerical simulation of the flow around a cylinder for $Ri = -1.0$:
 (a) Streamlines; (b) Isotherms.

6.1. CONCENTRATION OF A SUBSTANCE f IN A SQUARE DOMAIN

Concentration of a substance f in a square domain with a constant velocity field is analyzed using a dynamic adaptive mesh strategy, which is the main reason to present this case.

The computational domain and boundary conditions, as well as the prescribed velocity are shown in Fig. 7a. At points A and B, where the straight segment intersect the boundaries, it is taken $f=0.5$. The initial value inside the domain is $f=0.0$. Although this problem is two-dimensional, it was applied a three dimensional model taking one layer of elements in the normal direction to the plane formed by the axis x and y . Then, the initial mesh, with 2180 nodes and 6228 tetrahedral elements, is shown in Fig. 7b. The Peclet number, as defined by Raithby (1976), is given by $Pe=rU\Delta x/D$, where r is the specific mass, U is the velocity, D is the diffusion coefficient and Δx is a characteristic length, which was taken as 0.1 of the length of the computational domain.

As the main objective of this simple example is to show the behaviour of the dynamic mesh adaptation technique, only the case where $Pe = 20$ and $q=45^\circ$ is shown here. Only the concentration gradient indicator (see Popiolek and Awruch, 2006) with $a=0.0$ in Eq. (1) was used.

In Figure 8 a sequence of adaptive meshes, with the corresponding isolines of the substance concentration, at different times is presented, showing that the refinement/de-refinement procedure follows the solution along the time.

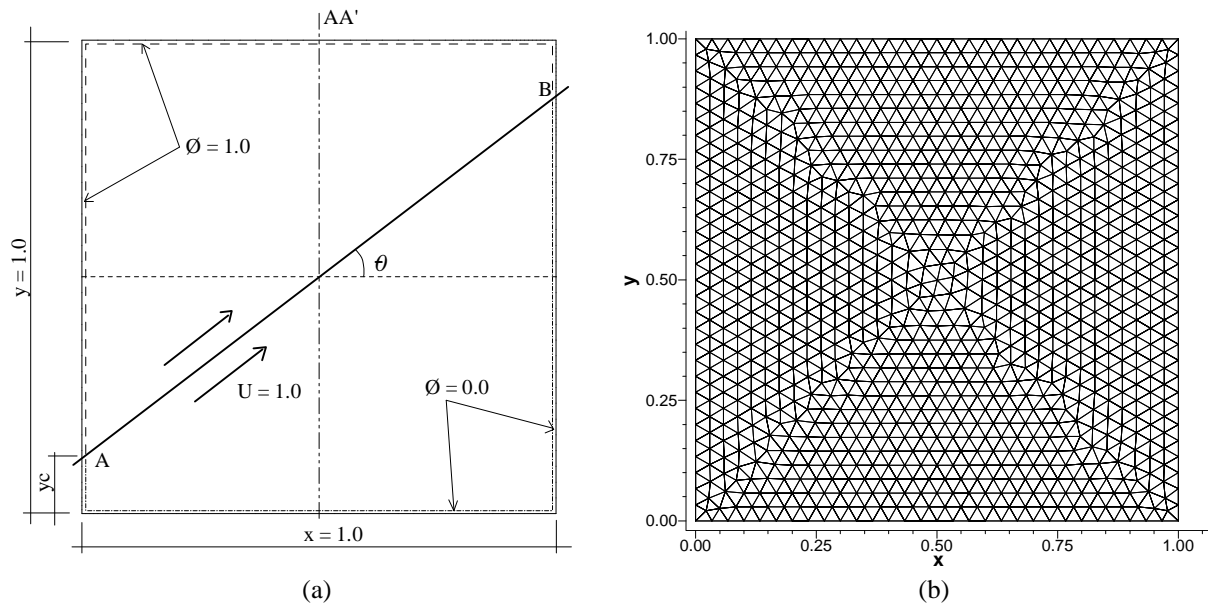


Figure 7. (a) Computational domain and boundary conditions. (b) Initial Mesh.

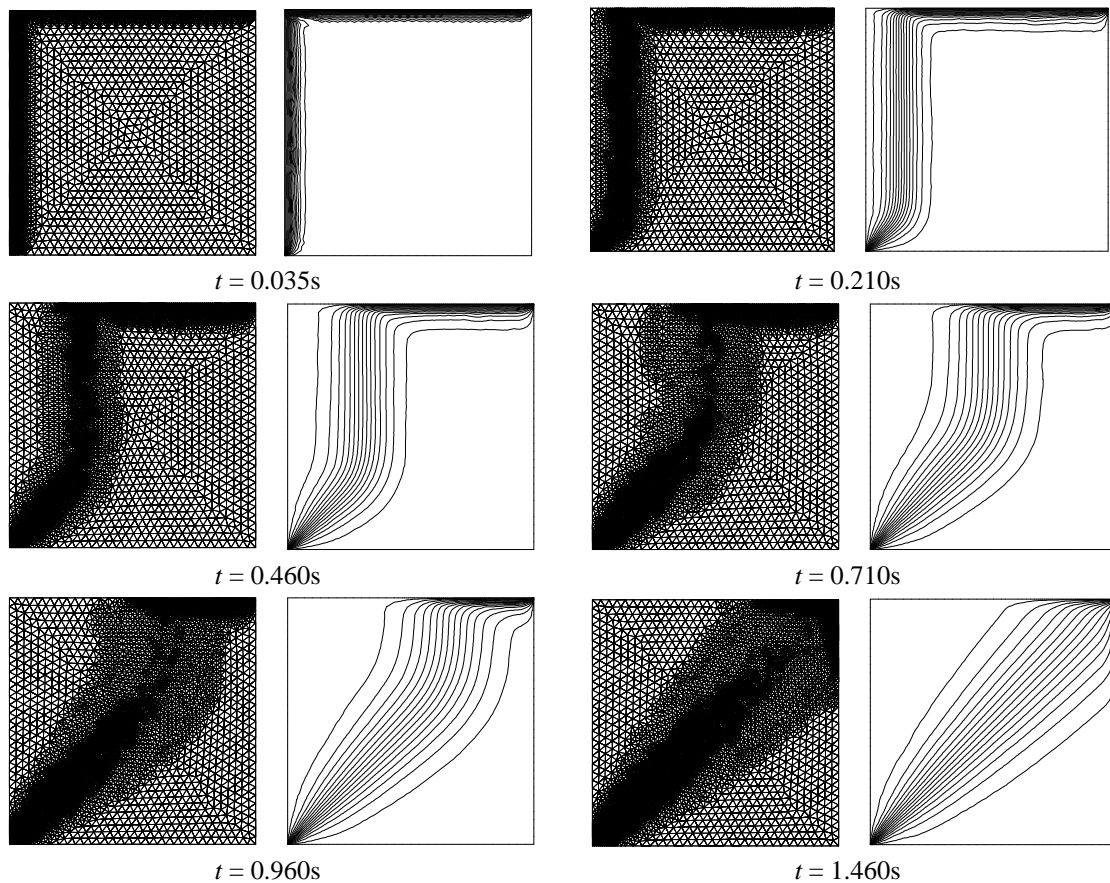


Figure 8 – Sequence of adaptive meshes and isolines of substance concentration at different times.

Mesh refinement were performed using uniform time intervals. This procedure was applied twice in the same time level and the initial mesh, with upload values of the variables, was taken as the basic grid to be refined each $\Delta t = 0.025$ s.

The concentration profile in section AA' ($x = 0.5$) and its comparison with the analytical solution given by Raithby (1976) are presented in Fig. 9 and good agreement was obtained. In Fig. 10 the concentration field, when steady state is reached, can be observed.

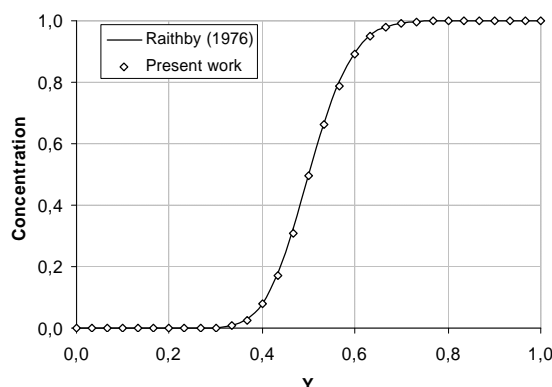


Figure 9. Concentration profile, in $x = 0.5$, for $q = 45^\circ$ and $Pe = 20$.

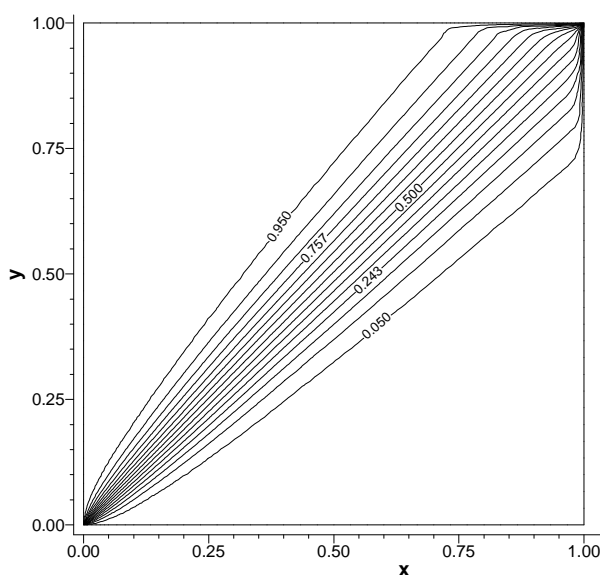


Figure 10. Isolines of the substance concentration, for $q = 45^\circ$ and $Pe = 20$.

5. CONCLUSIONS

An adaptive mesh strategy for the numerical simulation of incompressible transient flows with heat transfer and mass transport was used in order to improve the numerical solution accuracy. An Error indicator, an adaptation criterion, a refinement scheme, a smoothing process and an appropriate data structure are used to get a correct mesh.

The Finite Element technique, with unstructured meshes formed by tetrahedral elements and the two-step Taylor-Galerkin method was used. The velocity field was obtained by an explicit scheme, while pressure field was computed by an implicit scheme using a pre-conditioned conjugate gradient method.

Based on the results obtained in this work, it may be concluded that *regular* and *irregular* refinements have produced meshes consistent and useless refinement propagations have not been generated and the meshes adaptation following the temperature/concentration gradients, carrying through the refinements with fidelity.

Summarizing, the main contribution of the work are the formulation and application of a adaptive mesh strategy, which is integrated with an algorithm to simulate transient viscous incompressible flows, including heat transfer and mass transport.

6. REFERENCES

Ait-Ali-Yahia, D., Habashi, W.G., Tam, A., Vallet, M-G. and Frotin, M., 1996, A directionally adaptive methodology using an edge-based error estimate on quadrilateral grids, *International Journal for Numerical Methods in Fluids*, vol. 23, pp. 673-690.

- Argyris, J., Doltsinis, T.S. and Friz, H., 1990, Studies on computational reentry aerodynamics, *Computer Methods in Applied Mechanics Engineering*, vol. 81, pp. 257-187.
- Bank, R.E., Sherman, A.H. and Weise, A., 1983, Refinement algorithms and data structures for regular local mesh refinement, *Scientific Computing*, pp. 3-17.
- Bey, J., 1995, Tetrahedral grid refinement, *Computing*, vol. 55, pp. 355-378.
- Biswas, R. and Srawn, R.C., 1994, A new procedure for dynamic adaption of three-dimensional unstructured grid, *Applied Numerical Mathematics*, vol. 13, pp. 437-452.
- Connell, S.D. and Homes, D.G., 1994, Three-dimensional unstructured adaptive multigrid scheme for the Euler equations, *AIAA Journal*, vol. 32(8), pp. 1626-1632.
- Dannelongue, H.H. and Tanguy, P.A., 1990, Efficient data structures for adaptive remeshing with the FEM, *Journal of Computations Physics*, vol. 91, pp. 94-109.
- Demkowicz, L., Oden, J.T., Rachowicz, W. and Hardy, O., 1991, An h-p Taylor-Galerkin element method for compressible Euler equations, *Computer Methods in Applied Mechanics and Engineering*, vol. 88, pp. 363-396.
- Devloo, P., Oden, J.T. and Tattani, P., 1988, An h-p adaptive finite element method for the numerical simulation of compressible flow, *Computer Methods in Applied Mechanics and Engineering*, vol. 70, pp. 203-235.
- Freitag, L. A. and Ollivier-Gooch, C., 1996, A comparison of tetrahedral mesh improvement techniques, 5th International Meshing Roundtable, Pittsburgh, Pennsylvania, U.S.A., pp. 87-100.
- Grosso, R., Lürig, C. and Ertl, T., 1997, The multilevel finite element method for adaptive mesh optimization and visualization of volume data, *IEEE*, vol. 97, pp. 387-394.
- Hatanaka, K. and Kawahara, M., 1995, A numerical study of vortex shedding around a heated/cooled circular cylinder by the three-step Taylor-Galerkin method, *International Journal for Numerical Methods in Fluids*, vol. 21, pp. 857-867.
- Habashi, W.G, Dompierre, J., Bourgault, Y., Ait-ali-Yahia, D., Fortin M. and Vallet, M-G., 2000, Anisotropic mesh adaptation: toward user-independent, mesh independent and solver-independent CFD. Part I: general principles, *International Journal for Numerical Methods in Fluids*, vol. 32, pp. 725-744.
- Ivanenko, S.A and Azarenok, B.N., 2002, Application of moving adaptive grids for numerical solution of 2D nonstationary problems in gas dynamics, *International Journal for Numerical Methods in Fluids*, vol. 39, pp. 1-22.
- Kallinderis, Y. and Vijayan, P., 1993, Adaptive refinement-coarsening scheme for three-dimensional unstructured meshes, *AIAA Journal*, vol. 31(8), pp. 1440-1447.
- Löhner, R., 1987, An adaptive finite element scheme for transient problems in CFD, *Computer Methods in Applied Mechanics and Engineering*, vol. 61, pp. 323-338.
- Löhner, R., 1989, Adaptive remeshing for transient problems, *Computer Methods in Applied Mechanics and Engineering*, vol. 75, pp. 195-214.
- Mavriplis, D.J., 2000, Adaptive meshing technique for viscous flow calculations on mixed element unstructured meshes, *International Journal for Numerical Methods in Fluids*, vol. 34, pp. 93-111.
- Mavriplis, D.J., 1995, Unstructured mesh generation and adaptivity, ICASE.
- Peraire, J., Vahdati, M., Morgan, K. and Zienkiewicz, O.C., 1987, Adaptive remeshing for compressible flow computations, *Journal of Computations Physics*, vol. 72, pp. 449-466.
- Popiolek, T.L. and Awruch, A.M., 2006, Numerical simulation of incompressible flows using adaptive unstructured meshes and pseudo-compressibility hypothesis, *Advances in Engineering Software*, vol. 37, pp. 260-274.
- Probert, J., Hassan, O., Peraire, J. and Morgan, K., 1991, An adaptive finite element method for transient compressible flows, *International Journal for Numerical Methods in Engineering*, vol. 32, pp. 1145-1159.
- Raithby, G.D., 1976, Skew upstream differencing schemes for problems involving fluid flow, *Computer Methods in Applied Mechanics and Engineering*, vol. 9, pp. 153-164.
- Speares, W. and Berzins M., 1997, A 3D unstructured mesh adaptation algorithm for time-dependent shock-dominated problems, *International Journal for Numerical Methods in Fluids*, vol. 25, pp. 81-104.
- Zienkiewicz, O.C. and Wu, J., 1992, A general explicit of semi explicit algorithm for compressible and incompressible flows, *International Journal for Numerical Methods in Engineering*, vol. 35, pp. 457-479.
- Zienkiewicz, O.C., Mithiarasu, P., Codina, R., Vazquez, M. and Ortiz, P., 1999, The characteristic-based-split procedure: an efficient and accurate algorithm for fluid problems, *International Journal for Numerical Methods in Fluids*, vol. 31, pp. 359-392.
- Zhou, T., Shimada, k., 2000, An angle-based approach to two-dimensional mesh smoothing, 9th International Meshing Roundtable, New Orleans, Louisiana, USA, pp. 373-384.